Izv. VUZ. «AND», vol.11, № 3, 2003

ANALYTICAL DESCRIPTION OF RECURRENCE PLOTS OF WHITE NOISE AND CHAOTIC PROCESSES

M. Thiel, M.C. Romano, J. Kurths

We present an analytical description of the distribution of diagonal lines in Recurrence Plots for white noise and chaotic systems, and find that the latter one is linked to the correlation entropy. Further we identify two scaling regions in the distribution of diagonals for oscillatory chaotic systems that are hinged to two prediction horizons and to the geometry of the attractor. These scaling regions cannot be observed with the Grassberger-Procaccia algorithm. Finally, we propose methods to estimate dynamical invariants from RPs.

Dedicated to the 60th Birthday of Prof. Dr. Vadim Anishchenko

1. Introduction

Recurrence constitutes a fundamental property of dissipative chaotic systems. As Poincaré showed in his recurrence theorem in 1890 [1], if a system restricts its dynamics to a bounded subset of the phase space, the system will almost certainly, i.e. with probability one with respect to the natural measure, return arbitrarily close to any given initial condition.

Recurrence Plots (RPs) visualize in a two-dimensional binary matrix the recurrences of the system in phase space. The Recurrence Quantification Analysis (RQA) quantifies structures found in RPs to yield a deeper understanding of the underlying process from a given time series [2,3]. However, this method is widely applied [4 - 10] but in a rather pragmatic way. First steps in the direction of an analytical description were made by Faure et al. [11], Gao and Cai [3] and Casdagli [12].

In this contribution we give an analytical expression for the distribution of diagonals in RP in the case of stochastic processes and extend the results of [11,3] to chaotic flows. Further we compare our approach with the well-known Grassberger-Procaccia (G-P) algorithm [13] and show some advantages of the RP method for the estimation of some invariants of the dynamics, such as the correlation entropy. One of the most remarkable differences between our approach and the G-P algorithm is that we find two different scaling regions for oscillating chaotic flows, such as the Rössler system, instead of the single one obtained with the G-P algorithm. This new scaling region can be linked to the geometry of the attractor and defines another characteristic time scale of the system. Beyond we propose optimized measures for the identification of relevant structures in the RP.

The outline of this paper is as follows. In Sec. 2 we briefly introduce RPs. After considering in Sec. 3 the RPs of white noise, we proceed to general chaotic system (Sec. 4). Then, we exemplify our theoretical results for the Rössler system (Sec. 5) and present the two different scaling regions that characterize the system. Finally, we propose to estimate main characteristics of nonlinear systems from RPs which extends the importance of the RQA (Sec. 6).

2. Recurrence Plots and Recurrence Quantification Analysis

RPs were introduced to simply visualize the behavior of trajectories in phase space [2]. Suppose we have a dynamical system represented by the trajectory $\{\vec{x}_i\}$ for $i=1,\ldots,N$ in a d-dimensional phase space. Then we compute the matrix

$$R_{i,j} = \Theta(\varepsilon - |\vec{x}_i - \vec{x}_j|), \quad i,j = 1 \ldots N, \tag{1}$$

where ε is a predefined threshold and $\Theta(\cdot)$ is the Heaviside function[1]. The graphical representation of $R_{i,j}$, called Recurrence Plot, is obtained encoding the value one as «black» and zero as «white» point. A homogeneous plot with mainly single points may indicate a mainly stochastic system. Paling away from the main diagonal may indicate a drift i.e. non-stationarity of the time series. A main advantage of this method is that it allows to apply it to nonstationary data [4].

To quantify the structures that are found in RPs, the Recurrence Quantification Analysis (RQA) was proposed [6]. There are different measures that can be considered in the RQA. One crucial point for these measures is the distribution of the lengths of the diagonal lines $P_\varepsilon(l)$ that are found in the plot. In the case of deterministic systems the diagonal lines mean that trajectories in the phase space are close to each other on time scales that correspond to the lengths of the diagonals. In the next sections we show that there is a relationship between $P_\varepsilon(l)$ and the correlation entropy. On the other hand we compute the distribution of diagonals for random processes to see that even in this case, there are some diagonals which can lead to pitfalls in the interpretation of the RQA because noise is inevitable in experimental systems. A more detailed discussion of this problem is given in [14].

3. Results for white noise

In this section we compute analytically the probability to find a black or recurrence point and the distribution of diagonals of length l in the RP in the case of independent noise. The probability to find a recurrence point in the RP is given by

$$P_b(\varepsilon) = \lim_{N\to\infty} 1/N^2 \Sigma_{i,j=1}^{N} R_{i,j}, \tag{2}$$

and the probability to find a diagonal of at least length l in the RP is defined as

$$P_\varepsilon^c(l) = \lim_{N\to\infty} 1/N^2 \Sigma_{i,j=1}^{N} \prod_{m=0}^{l-1} R_{i+m,j+m}, \tag{3}$$

where c stands for cumulative. Note that $P_b(\varepsilon) = P_\varepsilon^c(1)$.

---

[1] The norm used in Eq. 1 is in principle arbitrary. For theoretical reasons, that we will present later, it is preferable to use the maximum norm. However the numerical simulations of this paper are based on the Euclidian norm to make the results comparable with the literature. The theoretical results of this paper hold for both choices of the norm.

We consider a random variable X with probability density $\rho(x)$. Suppose that $\{x_i\}$ for $i=1,\ldots,N$ is a realization of X and we are interested in the distribution of the distances of each point to all other points of the time series. This can be done by computing the convolution of the density $\rho(\cdot)$

$$R(x) = \rho(x)*\rho(x). \tag{4}$$

$P_b(\varepsilon)$ is then gained by integrating $R(x)$ over $[-\varepsilon,\varepsilon]$

$$P_b(\varepsilon) = \int_{-\varepsilon}^{\varepsilon} R(x)dx = 2\int_0^{\varepsilon} R(x)dx. \tag{5}$$

Note that $P_b(\varepsilon)$ is invariant against shuffling of the data. For [0,1] uniformly distributed noise, $R(x)$ is given by

$$R(x) = \begin{cases} 1 - |x| & \text{if } |x| < 1 \\ 0 & \text{else} \end{cases} \tag{6}$$

and hence the probability $P_b(\varepsilon)$ for RPs and CRPs is given by

$$P_b(\varepsilon) = 2\varepsilon - \varepsilon^2 + \Theta(\varepsilon-1)[1-2\varepsilon+\varepsilon^2]. \tag{7}$$

For Gaussian white noise one finds $P_b(\varepsilon)=\mathrm{erf}(\varepsilon/(2\sigma))$, where σ is the standard deviation.

Now it is straightforward to compute $P_\varepsilon^c(l)$ in the CRPs (in RPs only asymptotically). As the noise is independent, we obtain

$$P_\varepsilon^c(l) = P_b(\varepsilon)^l. \tag{8}$$

The probability to find a recurrence point $P_b(\varepsilon)$ is in both RPs and CRPs independent of the preceding point on the diagonal (except in the main diagonal). Eq. (8) shows that the probability to find a line of length l decreases exponentially with l.

For our example of uniformly distributed noise we get

$$P_\varepsilon^c(l) = (2\varepsilon-\varepsilon^2+\Theta(\varepsilon-1)[1-2\varepsilon+\varepsilon^2])^l. \tag{9}$$

Note that in this case the exponential decay depends on ε. Hence the larger ε, the longer are the diagonal lines that one obtains. Usually one analyses the RP computed with only one threshold ε. As long diagonals are interpreted as a deterministic feature of the system (good predictability), using only one ε can lead to a misinterpretation of the dynamics of the system.

In the next sections we will show that the distribution of diagonals decays also exponentionally for chaotic systems, but the decay is - at least in some region - independent of the threshold ε.

4. Results for chaotic systems

We present in this section an approach for chaotic systems. It is an extension of the results presented in [11] for chaotic maps and also covers general chaotic flows. To estimate the distribution of the diagonals in the RP, we start with the correlation integral [15]

$$C(\varepsilon) = \lim_{N\to\infty} 1/N^2 \times \{\text{number of pairs } (i,j) \text{ with } |\vec{x}_i - \vec{x}_j| < \varepsilon\}. \tag{10}$$

Note that the definition of $P_b(\varepsilon)$ coincides with the definition of the correlation integral

$$C(\varepsilon) = \lim_{N\to\infty} 1/N^2 \Sigma_{i=1}^{N} \Theta(|\vec{x}_i - \vec{x}_j| - \varepsilon) \overset{\text{Eq. 1}}{=} \lim_{N\to\infty} 1/N^2 \Sigma_{i,j=1}^{N} R_{i,j} = P_b(\varepsilon). \quad (11)$$

This fact allows to link the known results about the correlation integral to the structures in RPs.

We consider a trajectory $\vec{x}(t)$ in the basin of an attractor in the d-dimensional phase space and the state of the system is measured at time intervals τ. Let $\{1,2,...,M(\varepsilon)\}$ be a partition of the attractor in boxes of size ε. Then $p(i_1,...,i_l)$ denotes the joint probability that $\vec{x}(t=\tau)$ is in the box i_1, $\vec{x}(t=2\tau)$ is in the box i_2,..., and $\vec{x}(t=l\tau)$ is in the box i_l. The order-2 Rényi entropy [16,17] is then defined as

$$K_2 = -\lim_{\tau\to 0}\lim_{\varepsilon\to 0}\lim_{l\to\infty} 1/(l\tau) \ln \Sigma_{i_1,\ldots,i_l} p^2(i_1,\ldots,i_l). \quad (12)$$

We can approximate $p(i_1,\ldots,i_l)$ by the probability $P_{t,l}(\vec{x}, \varepsilon)$ of finding a sequence of points in boxes of length ε about $\vec{x}(t=\tau)$, $\vec{x}(t=2\tau)$, ..., $\vec{x}(t=l\tau)$. Assuming that the system is ergodic, which is always the case for chaotic systems as they are mixing, we obtain

$$\Sigma_{i_1,\ldots,i_l} p^2(i_1,\ldots,i_l) = 1/N \Sigma_{t=1}^{N} p_t(i_1,\ldots,i_l) \sim 1/N \Sigma_{t=1}^{N} P_{t,l}(\vec{x}, \varepsilon), \quad (13)$$

where $p_t(i_1,\ldots,i_l)$ represents the probability of being in the box i_1 at time $t=\tau$, in the box i_2 at time $t=2\tau$, ... and in the box i_l at time $t=l\tau$. Further we can express $P_{t,l}(\vec{x}, \varepsilon)$ by means of the recurrence matrix

$$P_{t,l}(\vec{x}, \varepsilon) = 1/N \Sigma_{s=1}^{N} \prod_{m=0}^{l-1} \Theta(\varepsilon - |\vec{x}_{t+m} - \vec{x}_{s+m}|) = 1/N \Sigma_{s=1}^{N} \prod_{m=0}^{l-1} R_{t+m,s+m}. \quad (14)$$

Hence we obtain an estimator for the order-2 Rényi entropy by means of the RP

$$\hat{K}_2(\varepsilon,l) = 1/(l\tau) \ln \underbrace{(1/N^2 \Sigma_{t,s=1}^{N} \prod_{m=0}^{l-1} R_{t+m,s+m})}_{(*)}. \quad (15)$$

Note that (*) is the cumulative distribution of diagonal lines $P_\varepsilon^c(l)$ (Eq. (3)). Therefore, if we represent $P_\varepsilon^c(l)$ in a logarithmic scale versus l we should obtain a straight line with slope $-\hat{K}_2(\varepsilon)\tau$ for large l's.

On the other hand, in the G-P algorithm the l-dimensional correlation integral is defined as

$$C_l(\varepsilon) = \lim_{N\to\infty} 1/N^2 \Sigma_{t,s=1}^{N} \Theta(\varepsilon - (\Sigma_{k=0}^{l-1} |\vec{x}_{i+k} - \vec{x}_{j+k}|^2)^{1/2}). \quad (16)$$

Grassberger and Procaccia [18] state that due to the exponential divergence of the trajectories, requiring

$$\Sigma_{k=0}^{l-1} |\vec{x}_{i+k} - \vec{x}_{j+k}|^2 \le \varepsilon^2 \quad (17)$$

is essentially equivalent to

$$|\vec{x}_{i+k} - \vec{x}_{j+k}| < \varepsilon \quad \text{for } k = 1,\ldots,l \quad (18)$$

which leads to the ansatz:

$$C_l(\varepsilon) \sim \varepsilon^{\nu} \exp(-l\tau K_2). \quad (19)$$

Further they make use of Takens embedding theorem [19] and reconstruct the whole trajectory from l measurements of any single coordinate. Hence they consider

$$\tilde{C}_l(\varepsilon) = \lim_{N\to\infty} 1/N^2 \Sigma_{t,s=1}^{N} \Theta(\varepsilon - (\Sigma_{k=0}^{l-1} |x_{i+k} - x_{j+k}|^2)^{1/2}) \quad (20)$$

and use the same ansatz Eq. (19) for $\tilde{C}_l(\varepsilon)$. Then, the G-P algorithm obtains an estimator of K_2 considering

$$\tilde{K}_2(\varepsilon,l) = 1/\tau \ln (\tilde{C}_l(\varepsilon)/\tilde{C}_{l+1}(\varepsilon)). \quad (21)$$

Due to the similarity of the RP approach to the G-P one, we state

$$P_\varepsilon^c(l) \simeq \Sigma_{i_1,\ldots,i_l} p^2(i_1,\ldots,i_l) \simeq \tilde{C}_l(\varepsilon) \sim \varepsilon^\nu \exp(-l\tau K_2). \quad (22)$$

The difference between both approaches is that in $P_\varepsilon^c(l)$ we further consider information about l vectors, whereas in $\tilde{C}_l(\varepsilon)$ we have just information about l coordinates. Besides this, in the RP approach l is a length in the plot, whereas in the G-P algorithm it means the embedding dimension. As K_2 is defined for $l\to\infty$, the RP approach seems to be more appropriate than the G-P one, as it is always problematic to use very high embedding dimensions [20].

A further advantage of the RP method is that it does not make use of the approximation that Eq. (17) is essentially equivalent to Eq. (18). The quantity that enters the RPs is directly linked to the conditions Eq. (18) and hence uses one approximation less than the G-P method.

One open question for both methods is the identification of the scaling regions. It is somewhat subjective and makes a rigorous error estimation problematic. For the cases considered in this paper we have found that 10,000 data points assure reliable results for both methods. Even 5,000 data points allow for a reasonable estimation, whereas 3,000 data points or less yield small scaling regions that are difficult to identify. However, the RP method is advantageous for the estimation of K_2 as the representation is more direct. The most important advantage is presented in the next section: RPs allow to detect another scaling region in the Rössler attractor that cannot be observed with the G-P algorithm.

5. The Rössler System

We analyze the Rössler system with standard parameters a=b=0.2, c=5.7 [21]. We generate 15,000 data points based on the Runge-Kutta method of fourth order and neglect the first 5,000. The integration step is h=0.01 and the sampling rate is 20.

First, we estimate K_2 by means of the G-P algorithm. Fig. 1 shows the results for the correlation integral in dependence on ε. There is one well-expressed scaling region for each embedding dimension l>3. Then we get from the vertical distances between the lines an estimate of $\tilde{K}_2$ (Fig. 2), K_2=0.070±0.003. Next, we calculate the cumulative distribution of the diagonal lines of the RP in dependence on the length of the lines l. We then represent the number of diagonals of length l, i.e. $N^c(l)$=N^2×$P_\varepsilon^c(l)$, where N is the length of the time series (Fig. 3). For large l and small ε the scaling breaks down as there are not enough lines in the RP. The most remarkable fact obtained here is the existence of two well differentiated scaling regions. The first one is found for $1\le l\le 84$ and the second one for $l\ge 85$. The existence of two scaling regions

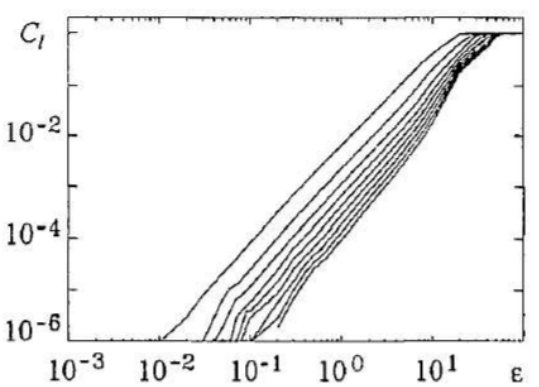

Fig. 1. G-P algorithm for the Rössler system; l varies from 3 (top) to 27 (bottom) in steps of 3

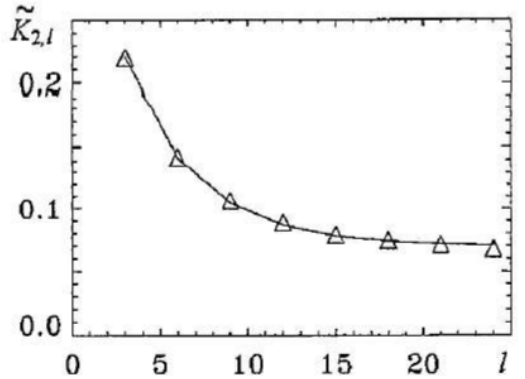

Fig. 2. Estimation of $\tilde{K}_{2,l}$ for the Rössler system with the G-P algorithm. The line is plotted to guide the eye

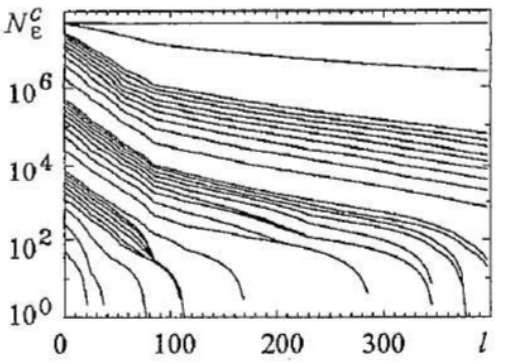

Fig. 3. Number of diagonal lines of at least length l in the RP of the Rössler system ($N^c(l)=N^2\times P_\varepsilon{}^c(l)$, where N is the length of the time series); ε varies logarithmically from 10^{-2} to 10.0 (bottom to top)

is a new and striking point obtained from this analysis and is not observed with the G-P method. The estimate of K_2^f from the slope of the first part of the lines is $K_2^f \approx 0.225 \pm 0.03$ (Fig. 4) and the one from the second part is $K_2 \approx 0.0675 \pm 0.004$ (Fig. 5). Hence, K_2^f is

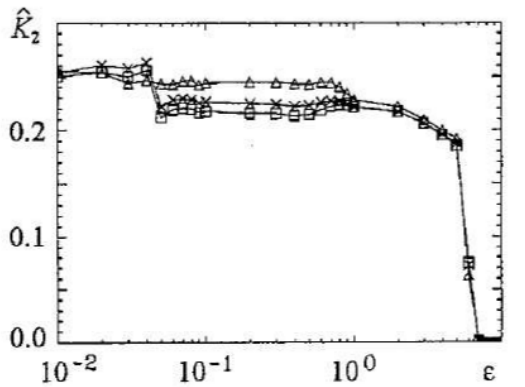

Fig. 4. RP method for the Rössler system: slope of the curves $N_\varepsilon{}^c(l)$ in the first region for three different choices (×:$l\in$[1,84], △:$l\in$[1,40], □ : $l\in$[16,80]) of the scaling region in l

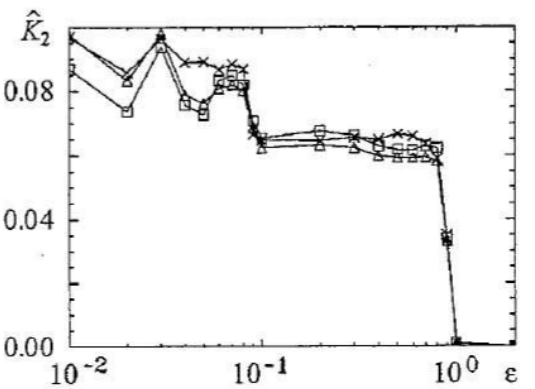

Fig. 5. RP method for the Rössler system: slope of the curves $N_\varepsilon{}^c(l)$ in the second region for three different choices (×: $l\in$[88,108], △: $l\in$ [88,200], □ : $l\in$[108,160]) of the scaling region in l

between 3-4 times higher than K_2. As K_2 is defined for $l\to\infty$, the second slope yields the estimation of the entropy.

However, the first part of the curve is interesting too, as it is also independent of ε. The region $1\le l\le 84$ characterizes the short term dynamics of the system up to three cycles around the fix point and corresponds in absolute units to a time of t=16.8, as we use a sampling rate of δt=0.2. These three cycles reflect a characteristic period of the system that we will call *recurrence period* T_{rec}. It is different from the dominant «phase period» T_{ph}, which is given by the dominant frequency of the power density spectrum. T_{rec} however, is given by recurrences to almost the same state in phase space.

Recurrences are represented in the plot by vertical (or horizontal, as the plot is symmetric) lines. Such a line occurs at the coordinates i, j if

$$R_{i,j+m} = \begin{cases} 1 & \text{if } m=-1 \\ 0 & \text{for } m\in\{0,\ldots,l-1\} \\ 1 & \text{if } m=l. \end{cases} \qquad (23)$$

The trajectory $\vec{x}_n$ for times $n=j-1,\ldots j+l$ is compared to the point $\vec{x}_j$. Then the structure given by Eq. (23) can be interpreted as follows. At time $n=j-1$ the trajectory falls within an ε-box of $\vec{x}_j$. Then for $n=j,\ldots j+l-1$ it moves outside of the box, until at $n=j+l$ it recurs to the ε-box of $\vec{x}_j$. Hence, the length of the line is proportional to the time that the trajectory needs to recur close to $\vec{x}_j$.

In Fig. 6 we represent the distribution of vertical lines in the RP. The period of about 28 points corresponds to T_{ph}. However, the highest peak is found at a lag of about 87 points (the second scaling region begins at l=85). This means that after this time most of the points recur close to their initial state. This time also defines the recurrence period T_{rec}. For the Rössler attractor with standard parameters we find $T_{rec}\approx 3T_{ph}$.

For predictions on time scales below the recurrence period, $\tau=1/K_2^f$ is a better estimate of the prediction horizon than $\tau=1/K_2$. This interesting result means that the possibility to predict the next value within an ε-range is in the first part by a factor of more than 3 times worse than it is in the second part, i.e. there exist two time scales that characterize the attractor. The first slope is greater than the second one because it is more difficult to predict the next step if we have only information about a piece the trajectory for less than one recurrence period. Once we have scanned the trajectory for more than T_{rec}, the predictability increases and the slope of $P_\varepsilon^c(l)$ in the logarithmic plot decreases. Hence the first slope, as well as the time scale at which the second slope begins, reveal important characteristics of the attractor.

To investigate how the length of the first scaling region depends on the form of the attractor, we have varied the parameter c of the Rössler system with fixed $a=b=0.1$, so that different types of attractors appear [22]. Especially we have studied the cases $c=9$, which yields $T_{rec}=2T_{ph}$, and $c=30$, which gives $T_{rec}=4T_{ph}$. In both cases the length of the first scaling region corresponds as expected to T_{rec}.

On the other hand, the existence of the two scalings may be linked to the amplitude fluctuations and the phase diffusion of the Rössler system, because the same two time scales have been also recently found by Anishchenko et al. based on a rather subtle method [23 - 25]. There, the first scaling region was linked to the amplitude fluctuations and the second one to the phase diffusion.

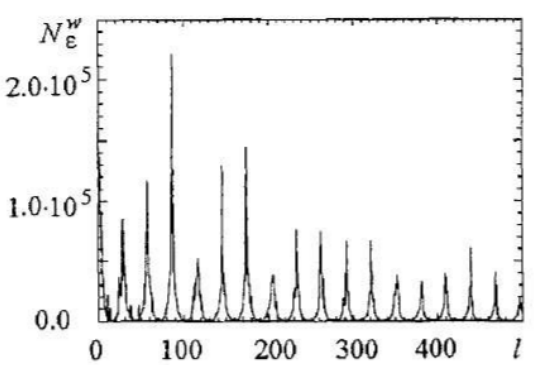

Fig. 6. Number of vertical lines in the Recurrence Plot of the Rössler system with standard parameters, ε=0.05 and based on 60,000 data points

The effect of the two scaling regions in the distribution of diagonal lines is also detectable in other oscillating nonhyperbolic systems like the Lorenz system and our simulations suggest a connection to the conclusions presented in [23]. We will report our results in more detail in a forthcoming paper.

6. Dynamical invariants for the RQA

With regard to our theoretical findings in Sec. 4 we have to assess the quality of the possible results of the RQA.

The measures considered in the RQA [6] are not invariants of the dynamical system, i.e. they usually change under coordinate transformations, and especially, they are in general modified by embedding [26]. Hence, we propose new measures to quantify the structures in the RP, that are invariants of the dynamical system.

The first measure we propose, is the slope of the cumulative distribution of the diagonals for large l. We have seen that it is (after dividing by τ) an estimator of the Rényi entropy of second order K_2, which is a known invariant of the dynamics [27]. On the other hand, we also can consider the slope of the distribution for small l's, as this slope shows a clear scaling region, too. The inverse of these two quantities, is then related to the forecasting time at different horizons. Especially the transition point from the first to the second scaling region is an interesting characteristic of the system.

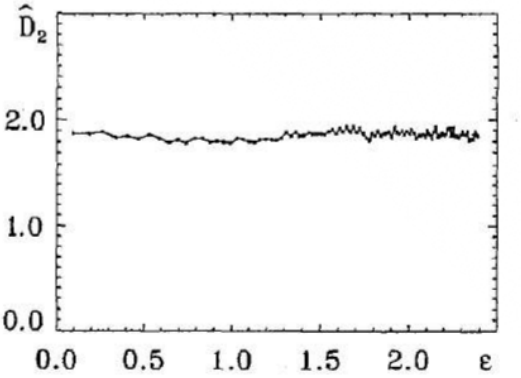

Fig. 7. Estimation of the correlation dimension D_2 for the Rössler attractor by the RP method. The parameters used for the Rössler system and the integration step are the same as in Sec. 5

The second measure we introduce, is the vertical distance between $P_\varepsilon^c(l)$ for different ε's. From Eq. (22) one can derive

$$\hat{D}_2(\varepsilon) = \ln(P^c_\varepsilon(l)/P^c_{\varepsilon+\Delta\varepsilon}(l))(\ln(\varepsilon/(\varepsilon+\Delta\varepsilon)))^{-1}. \tag{24}$$

This is an estimator of the correlation dimension D_2 [17]. The result for the Rössler system is represented in Fig. 7. The mean value of $\hat{D}_2(\varepsilon)$ is in this case 1.86±0.04. This result is in good accordance with the estimation of D_2 by the G-P algorithm given in [28], where the value 1.81 is obtained. With a modified G-P algorithm a value of 1.89 was reported [28].

The third measure we suggest, is an estimator of the generalized mutual information of order 2,

$$I_2(\tau) = 2H_2 - H_2(\tau) \tag{25}$$

where

$$H_2 = -\ln\Sigma_i p_i^2, \qquad H_2(\tau) = -\ln\Sigma_i p_{i,j}^2(\tau) \tag{26}$$

are the generalized Rényi's second order entropy (also correlation entropy) and its corresponding joint second order entropy [29]. This measure can be estimated using the G-P algorithm as follows [30]

$$\tilde{I}_2(\varepsilon,\tau) = \ln(C_2(\varepsilon,\tau)) - 2\ln(C_1(\varepsilon)). \tag{27}$$

Instead, we can estimate $I_2(\tau)$ using the recurrence matrix. As discussed in the preceding sections, one can estimate H_2 as

$$\hat{H}_2 = -\ln[1/N^2\Sigma_{i,j=1}^{N}R_{i,j}]. \tag{28}$$

Analogously we can estimate the joint second order entropy by means of the recurrence matrix

$$\hat{H}_2(\tau) = -\ln[1/N^2\Sigma_{i,j=1}^{N}R_{i,j}R_{i+\tau,j+\tau}]. \tag{29}$$

We compare the estimation of $I_2(\tau)$ based on the G-P algorithm with the one obtained by the RP method in Fig. 8. We see, that the RP method yields systematically higher estimates of the mutual information, as in the case of the estimation of the correlation entropy. However, the structure of the curves is qualitatively the same (it is just shifted to higher values by about 0.2). A more exhaustive inspection shows, that the difference is due to the use of the Euclidean norm. The estimate based on the RP method

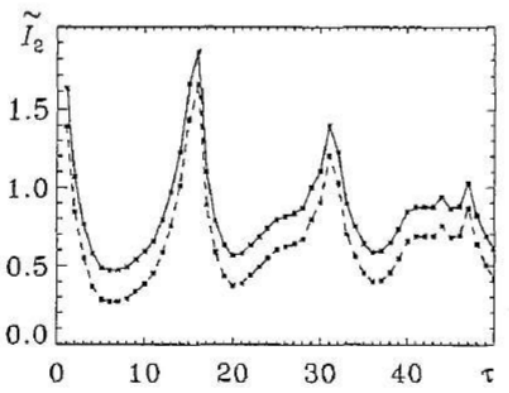

Fig. 8. Comparison of the estimators of the mutual information for the x-component of the Rössler system computed by the RP method (solid line) and the G-P algorithm (dashed line). The parameters used for the Rössler system and the integration step are the same as in Sec. 5

is almost independent of the norm, whereas the estimate based on the G-P algorithm clearly depends on the special choice. If the maximum norm is used (in G-P and RP) both curves coincide.

Note that the estimators for the invariants we propose are different from the ones of the G-P algorithm.

The three measures that we have proposed, are not only applicable for chaotic systems but also for stochastic ones, as the invariants are equally defined for both kinds of systems.

7. Conclusions

In this paper we have presented an analytical expression for the distribution of diagonals $P_\varepsilon(l)$ for stochastic systems and chaotic flows, extending the results presented in [11]. We have shown that $P_\varepsilon(l)$ is linked to the second order Rényi entropy rather than to the Lyapunov exponent. Further we have found in the logarithmic plot of $P_\varepsilon(l)$ two different scaling regions with respect to ε, that characterize the dynamical system and are also related to the geometry of the attractor. This is a new insight provided by RPs that cannot be seen by the G-P algorithm and will be studied in more detail in a forthcoming paper. The first scaling region defines a new time horizon for the description of the system for short time scales. Beyond the RP method does not make use of high embedding dimensions, and the computational effort compared with the G-P algorithm is decreased. Therefore the RP method is rather advantageous than the G-P one for the analysis of rather small and/or noisy data sets. Besides this, we have proposed different measures for the RQA, like estimators of the second order Rényi entropy K_2, the correlation dimension D_2 and the mutual information, that are, in contrast to the other often used RQA measures, invariants of the dynamics [26].

We thank Vadim Anishchenko very much for the long-standing and very exciting discussions and his suggestions on this work. Moreover we thank Dieter Armbruster, Annette Witt, Udo Schwarz and Norbert Marwan for the fruitful discussions. The project was supported by the «DFG Priority Program 1114».

References

1. *Poincaré H.* Sur le problème des trois corps et les équations de la dynamique // Acta Math. 13 (1890) 1-270.

2. *Eckmann J.-P., Kamphorst S.O. and Ruelle D.* Recurrence Plots of Dynamical Systems // Europhysics Letters.4 (1987) 973-977.

3. *Gao J. and Cai H.* On the structures and quantification of recurrence plots // Physics Letters.A 270 (1999) 75-87.

4. *Marwan N., Wessel N., Meyerfeldt U., Schirdewan A. and Kurths J.* Recurrence Plot Based Measures of Complexity and its Application to Heart Rate Variability Data // Phys. Rev. E.66 (2002) 026702.

5. *Marwan N., Kurths J.* Nonlinear analysis of bivariate data with cross recurrence plots // Phys. Lett. A.302(5-6) (2002) 299-307.

6. *Webber C.L. Jr. and Zbilut J.P.* Dynamical assessment of physiological systems and states using recurrence plot strategies // J. Appl. Physiol. 76 (1994) 965-973.

7. *Zbilut J.P., Giuliani A. and Webber C.L. Jr.* Recurrence quantification analysis and principal components in the detection of short complex signals // Physics Letters A 237 (1998) 131-135.

8. *Zbilut J.P., Giuliani A. and Webber C.L. Jr.* Detecting deterministic signals in exceptionally noisy environments using cross-recurrence quantification // Physics Letters A 246 (1998) 122-128.

9. *Holyst J.A., Zebrowska M. and Urbanowicz K.* Observations of deterministic chaos in financial time series by recurrence plots, can one control chaotic economy? // Eur. Phys. J. B 20 (2001) 531-535.

10. *Kurths J., Schwarz U., Sonett C.P. and Parlitz U.* Testing for nonlinearity in radiocarbon data // Nonlinear Processes in Geophysics 1 (1994) 72-75.

11. *Faure P. and Korn H.* A new method to estimate the Kolmogorov entropy from recurrence plots: its applications to neuronal signals // Physica D. 122 (1998) 265-279.

12. *Casdagli M.C.* Recurrence plots revisited // Physica D. 108 (1997), 12-44.

13. *Grassberger P. and Procaccia I.* Characterization of strange attractors // Phys. Rev. Lett. 50, number 5 (1983) 346-349.

14. *Thiel M., Romano M.C., Kurths J., Meucci R., Allaria E. and Arecchi T.* Influence of observational noise in recurrence quantification analysis // Physica D 171, number 3 (2002) 138-152.

15. *Grassberger P. and Procaccia I.* Measuring the strangeness of strange attractors // Physica D 9 (1983) 189-208.

16. *Rényi A.* Probability theory. North-Holland, (1970) (appendix).

17. *Grassberger P.* Generalized dimensions of strange attractors // Physics Letters 97 A, № 6 (1983) 227-230.

18. *Grassberger P. and Procaccia I.* Dimensions and entropies of strange attractors from a fluctuating dynamics approach // Physica D 13 (1984) 34-54.

19. *Takens F.* Detecting strange attractors in turbulence, in: Dynamical Systems and Turbulence / Eds. D.A. Rand and L.-S. Young // Lecture Notes in Mathematics, Vol. 898 (Springer, Berlin, 1980).

20. *Ruelle D.* Deterministic chaos: the science and the fiction // Proc. R. Soc. Lond. A, 427 (1990) 241-248.

21. *Rössler O.E.* An equation for continuous chaos // Phys. Lett. 57A, (1976) 397-398.

22. *Alligood K.T., Sauer T.D. and Yorke J.A.* Chaos an introduction to dynamical systems. Springer (1996).

23. *Anishchenko V.S., Vadivasova T.E., Kopeikin A.S., Strelkova G.I. and Kurths J.* Spectral and correlation analysis of spiral chaos // Fluctuation and Noise Letters, 3 (2003), L213-L221.

24. *Anishchenko V.S., Vadivasova T.E., Okrokvertskhov G.A. and Strelkova G.I.* Correlation analysis of dynamical chaos // Physica A 325 (2003), 199-212.

25. *Anishchenko V.S., Astakhov V., Neiman A., Vadivasova T. and Schimansky-Geier L.* Nonlinear Dynamics of Chaotic and Stochastic Systems. Springer (2001).

26. *Thiel M., Romano M.C. and Kurths J.* Spurious structures in Recurrence Plots induced by embedding // Chaos (submitted for publication).

27. *Schuster H.G.* Deterministic Chaos. Wiley VCH, (1984).

28. *Raab C. and Kurths J.* Estimations of large-scale dimensions densities // Phys. Rev. E 64 (2001) 0162161-0162165.

29. *Pompe B.* Measuring Statistical Dependences in a Time Series // J. Stat. Phys. 73 (1993), 587-610.

30. *Kantz H. and Schreiber T.* Nonlinear Time Series Analysis. University Press, Cambridge, (1997).

University of Potsdam, Germany *Received 28.08.2003*

УДК 519.6

АНАЛИТИЧЕСКОЕ ОПИСАНИЕ ОТОБРАЖЕНИЙ ПОСЛЕДОВАНИЯ ДЛЯ БЕЛОГО ШУМА И ХАОТИЧЕСКИХ ПРОЦЕССОВ

M. Thiel, M.C. Romano, J. Kurths

Дано аналитическое описание распределения диагональных линий в отображениях последования для белого шума и систем с хаотической динамикой; показано, что это распределение связано с корреляционной энтропией. Идентифицированы две области скейлинга в распределении диагоналей для колебательных систем с хаотической динамикой, которые тесно связаны с двумя горизонтами предсказуемости и с геометрией аттрактора. Эти области скейлинга не могут быть получены с помощью алгоритма Грассбергера - Прокаччиа. В заключение предложены методы определения динамических инвариантов из отображений последования.

Marco Thiel was born in 1974 in Paderborn (Germany). After finishing his diploma degree he started his PhD studies at the Nonlinear Dynamics group of Prof. Kurths at the University of Potsdam. E-mail: thiel@agnld.uni-potsdam.de

Maria Carmen Romano was born in 1975 in Tudela (Spain). She studied physics in the Universities of Zaragoza (Spain) and Paderborn (Germany). After finishing her diploma degree she started in 1999 her PhD studies at the Nonlinear Dynamics group of Prof. Kurths at the University of Potsdam.
E-mail: romano@agnld.uni-potsdam.de

Jürgen Kurths was born in GDR (1953). He graduated the University of Rostok (1975) in Mathematics and has got his PhD (1981). Now he is Director of the Interdisciplinary Center Dynamics of Complex Systems at the University of Potsdam, Full Professor (C4) for Theoretical Physics/Nonlinear Dynamics at University of Potsdam, Vice speaker of Sonderforschungsbereich Komplexe Nichtlineare Prozesse (Deutsche Forschungs-gemeinschaft), Vice President of the European Geophysical Society, Coordinator EU Network «Control, Synchronization and Characterization of Spatially Extended Nonlinear Systems». He is the member of the Editorial Board of Int. J. Bifurcation and Chaos, Visiting Fellow Muroran Institute of Technology (2001, Japan). J. Kurths is the Fellow of Fraunhofer Society, Guest Fellow of Max-Planck-Society, Fellow of the American Physical Society. E-mail: JKurths@agnld.uni-potsdam.de